Available online at www.sciencedirect.com
SCIENCE DIRECT®
Journal of Magnetic Resonance 167 (2004) 97–106
JMR Journal of Magnetic Resonance
www.elsevier.com/locate/jmr

Diffusion in porous building materials with high internal magnetic field gradients

J. Petković, H.P. Huinink, L. Pel,* and K. Kopinga*

Department of Applied Physics, Eindhoven University of Technology, P.O.Box 513, 5600 MB Eindhoven, The Netherlands

Received 5 June 2003; revised 4 November 2003

Abstract

Measuring the water diffusivity in porous building materials with NMR is hindered by the presence of large internal magnetic field gradients originating from magnetic impurities (Fe). To investigate the diffusion of water in these materials, a stimulated echo NMR technique is applied. A new analytical equation for the long-time signal decay in the presence of spatially varying internal field gradients is derived. This equation is experimentally confirmed by measurements on representative materials with large internal gradients (fired-clay brick and sintered crushed glass) and a material with very small internal gradients (glass filter). The diffusivity is determined in the long time limit, where it is constant and limited by the tortuosity of the pore structure. Tortuosities of different samples derived from the NMR data show an excellent agreement with the macroscopic tortuosities measured by electrochemical impedance spectroscopy. The developed technique can also be applied in unsaturated media, during e.g., drying, water absorption, and concentration changes. The characteristic length scales of the internal field fluctuations estimated from the model are compared with the structural length scales, whereas the magnitude of these fluctuations is compared with results of macroscopic magnetization measurements.

PACS: 82.56.Jn; 82.56.Lz; 82.56.Na

Keywords: NMR; Porous media; Diffusion; Internal field gradients

1. Introduction

In porous building materials, moisture and (dissolved) ions can give rise to several kinds of damage, e.g., frost damage, salt crystallization, corrosion of the reinforcement, and mould growth. Moisture and salt are naturally present in the materials, and their quantity is increased by atmospheric influence (rain), neighborhood of salt water, etc. Knowledge of the transport properties of moisture and salt is necessary to obtain information about the durability of building materials. In this paper we will study the diffusivity of the fluid in some representative building materials and relate it to structural parameters like the tortuosity [1].

NMR is a nondestructive technique that can be used for measuring the effective diffusivities of water, hydrocarbons, and ion species in porous materials [2–4]. The diffusivities obtained from these measurements are found to depend on the measurement time. With increasing times diffusing molecules start to feel the pore walls and the diffusion become restricted. From the measured time dependence of the diffusivity it is possible to obtain important structural information on the material [4,5]. From the results for short times, it is possible to obtain the surface-to-volume ratio and pore diameter, whereas for long times (order of seconds) the diffusivity is constant and limited by the tortuosity of the pore structure. Therefore NMR offers the possibility to determine the tortuosity of the pore system [6]. An alternative method to determine the tortuosity is electrochemical impedance spectroscopy, which is based on the measurement of the conductivity of ions dissolved in the pore fluid [7]. NMR is preferred when chemical

* Corresponding author. Fax: +31402473406.
E-mail addresses: l.pel@tue.nl (L. Pel), k.kopinga@tue.nl (K. Kopinga).

1090-7807/$ - see front matter © 2003 Published by Elsevier Inc.
doi:10.1016/j.jmr.2003.11.007

reactions or adsorption of ions at the pore walls occur, when the pore fluid already contains ions (cement and concrete) [8] and during monitoring of time-dependent processes, like drying or absorption. Especially in the unsaturated state of a material, the diffusivity of the dissolved ions, which is measured electrochemically, can no longer be related to the diffusivity, since the latter may contain an important contribution from transport by vapor diffusion.

Generally, NMR diffusion measurements are performed using pulsed field gradient (PFG) techniques [18]. By analyzing the NMR signal decay induced by PFGs, accurate results can be obtained when the internal field gradients are small. However, in many building materials a large amount of magnetic impurities (Mn, Fe, and Co) can be present, which may give rise to internal gradients that are at least an order of magnitude larger than the gradients that can be applied externally [9,10]. These gradients are often several orders of magnitude larger than the gradients induced by susceptibility differences between, e.g., water and a clean (diamagnetic) porous material. In fired-clay brick, for instance, the internal field gradients induced by the presence of about 4% Fe cause such a rapid dephasing of the transverse nuclear magnetization, that even down to echo spacings of 100 μs, CPMG measurements show very pronounced diffusion effects. Using Hahn spin-echo pulse sequences with varying echo time, we observed a decay of the spin-echo signal in this material by more than a factor of 100 within 10 ms. Within experimental inaccuracy, this decay was independent of the magnitude and direction of the applied field gradient (0.2–1 T/m).

Since our aim is to determine the diffusivity at times of the order of seconds, we have to use a pulse sequence in which the part of the nuclear magnetization that generates the relevant NMR signal is in the longitudinal direction during most of the measurement time, such as the stimulated-echo sequence [11]. This sequence has proven to be appropriate for diffusivity measurements in heterogeneous systems, but often very specialized pulse sequences like the '13-interval' sequence [12] have to be used, to suppress the effect of the cross terms between the internal and applied gradients [4–6,13], even if these gradients are small compared to the applied PFGs. It has been shown that at long observation times this approach may fail, since it is based on the assumption that the diffusing molecules experience a constant internal field gradient during the experiment [14]. In principle, the genuine diffusivities in heterogeneous media can be obtained by extrapolation of the data obtained from simple PFG stimulated-echo measurements [15]. This technique, however, has only been applied to systems with single-exponential signal decays, and may therefore not be suitable for our materials, which show pronounced multi-exponential decays [10].

In principle, the cross terms between the internal magnetic field fluctuations and the applied field gradients may be suppressed by using RF field gradients instead of B_0 gradients [16]. This may be an interesting alternative if the B_1 gradient can be made large enough to overcome the very large resonance offset fields present in magnetically 'dirty' materials. In this paper, however, we will focus on the question whether it is possible to apply a simple, constant field gradient NMR method to determine the diffusivity in such materials.

We will first define the characteristic length scales of pore structure and the internal magnetic fields. In this respect one should note that the distribution of the Fe impurities in our materials is not precisely known, and hence we will not a priory assume that both length scales are equal [17]. Next, we will introduce a new equation for the long-time stimulated-echo decay in materials with large internal gradients and confirm it experimentally for two materials with and one material without magnetic impurities. We will determine the diffusivity and quantitatively characterize the fluctuations of the internal magnetic fields. Finally, we will compare these results with data obtained by other methods.

2. NMR method

As already mentioned in Section 1, in porous media containing large amounts of magnetic impurities the transverse magnetization decays very fast, so it will have vanished at time scales at which the effect of the pore geometry on the diffusion of the water molecules can be observed. The stimulated-echo magnetization decay is governed by the longitudinal relaxation time (T_1) for a substantial part of the measurement time, during which it is in the longitudinal direction. Therefore T_2 and dephasing effects are minimized.

In Fig. 1 we have schematically plotted the pore structure of the material and the magnetic field fluctuations, together with their characteristic length scales. At long time scales molecules diffuse over distances longer than the correlation length of the medium ξ_S. The typical time scale related to ξ_S is $t_S \equiv \xi_S^2/6D$, where D is the diffusivity of the water molecules within the pore system. At length scales much larger than ξ_S the porous medium can be considered as homogeneous; the diffusivity D is constant and determined by the geometry of the pore system. This is often called the tortuosity limit [1]. The tortuosity of a medium is defined by the following relation:

$$\alpha = D_0/D, \tag{1}$$

where D_0 is the bulk (self) diffusion constant of the pore fluid.

The stimulated echo pulse sequence [11] is plotted schematically in Fig. 2. The signal attenuation for free

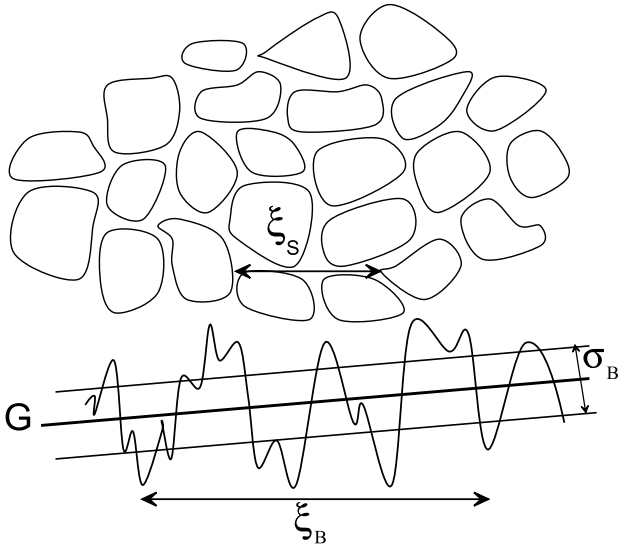

Fig. 1. Porous media characterized by a structural length scale ξ_S and a length scale ξ_B, associated with the fluctuations of the internal field. During the measurements a constant external gradient is applied. The internal field gradients are superimposed on these external gradients.

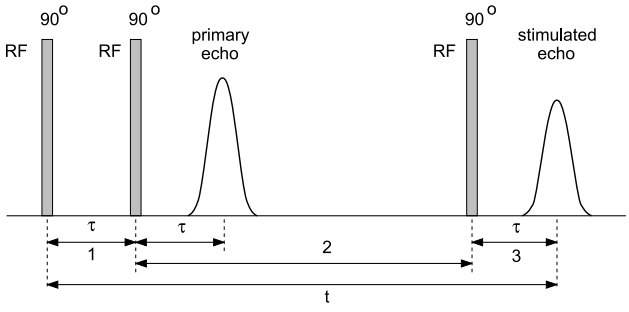

Fig. 2. Stimulated echo pulse sequence with a constant field gradient. The magnetization decay is measured by changing the time between the second and third RF pulse (period 2). Measurements are performed for different values of τ and the applied field gradient G.

diffusion is well known and can be described analytically. When the stimulated echo intensity M_{st} is divided by primary echo intensity M_{pr}, the following equation is obtained:

$$\ln(M_{st}/M_{pr}) = -[1/T_1 + (\gamma G)^2 D\tau^2]\, t. \quad (2)$$

In this equation T_1 is longitudinal relaxation time, γ is the gyromagnetic ratio (for a ^{1}H nucleus $\gamma = 2.67 \times 10^8\,\mathrm{rad\,s^{-1}\,T^{-1}}$), G is the applied external gradient, τ the time between the first two 90° pulses and t is stimulated-echo time. By dividing the two echo intensities the T_2 relaxation term is eliminated automatically.

Eq. (2) holds for diffusion in bulk liquids and for diffusion in a macroscopically isotropic porous medium on length scales larger than ξ_S, where the medium can be considered as homogenous (the tortuosity limit). When internal gradients are present, the initial signal decay is generally very fast, and cannot be described by Eq. (2). The internal fields can be characterized by a characteristic length scale ξ_B (Fig. 1). The typical time scale related to ξ_B is $t_B \equiv \xi_B^2/6D$. At time scales shorter than t_B, the internal fields experienced by a spin during the periods 1 and 3 of the stimulated-echo sequence (Fig. 2), when the magnetization is in transverse plane, are still correlated. For time scales much larger than t_B these internal fields become uncorrelated [18] and the spins experience a purely random internal field.

For these time scales ($t \gg t_B$) the magnetization decay can be described by the equation

$$\ln[M(t)/M_0] = -\gamma^2\tau^2\left\langle (\bar{B}_\tau)^2 \right\rangle - \left(T_1^{-1} + \gamma^2 G^2 \tau^2 D\right) t. \quad (3)$$

In this equation $\langle (\bar{B}_\tau)^2 \rangle$ is the ensemble average of $\bar{B}_\tau$, which is the temporal average of the internal field experienced by a spin during an interval τ (periods 1 and 3, Fig. 2). For very small τ, $\langle (\bar{B}_\tau)^2 \rangle$ becomes equal σ_B^2, the squared standard deviation of the internal field $\bar{B}$. For details of the derivation we refer to the Appendix A. In this derivation it was assumed that $\tau \ll T_2$, the transverse relaxation time.

Eq. (3) shows that the magnetization decay at long time scales can be described by a single exponent. This equation consists of three parts. The first term gives the total signal attenuation due to diffusion in the internal gradients. The second term is the contribution of the longitudinal relaxation. The third term describes the signal attenuation due to diffusion in the externally applied gradient. The important feature of the first term is that it does not depend on t, because the internal fields have become uncorrelated (spatially random) on the length scales much larger than ξ_B. With increasing echo times t, the second and third term of Eq. (3) become more important. At these times, decay due to diffusion is governed only by externally applied gradients and as such can be quantified.

From the right-hand side of Eq. (3) we are able to define a crossover time t^*

$$t^* \equiv \frac{\gamma^2\tau^2\left\langle (\bar{B}_\tau)^2 \right\rangle}{1/T_1 + (\gamma G)^2 D\tau^2}. \quad (4)$$

At time scales shorter than t^* the internal fields dominate the signal decay. At longer time scales ($t > t^*$) the longitudinal relaxation and dephasing due to the applied gradients start to play significant role. Therefore, the diffusivity D can only be measured when the signal is still above the noise level for $t > t^*$.

In a stimulated-echo experiment, the signal intensities of both the primary and the stimulated echo can be measured. In Eq. (2) the ratio of these two intensities is directly related to, amongst others, the diffusion coefficient D. On the other hand, Eq. (3) contains the ratio $M(t)/M_0$. In our experiments, this ratio is not necessarily equal to M_{st}/M_{pr}. The reasons for this are 2-fold.

First, a significant dephasing of the transverse components of the magnetization forming the primary echo may occur during the time interval between the first and second 90° pulse, which is not completely refocused at the time of the primary echo, due to the diffusive motion of the spins in the large local field inhomogeneities. Second, even if complete refocusing would occur, M_{st}/M_{pr} would only be equal to $M(t)/M_0$ for perfect 90° pulses. Since our samples are often much larger than thickness of the slices selected by our RF pulses (see Section 3), this condition is generally not satisfied in our experiments. However, we measure the decay of the stimulated echo for a constant value of τ, and hence for a constant intensity of the primary echo. Since, on the other hand, only one coherent pathway contributes to the stimulated echo, the only effect of using M_{st}/M_{pr} instead of $M(t)/M_0$ in Eq. (3) is the introduction of a constant scaling factor. This was checked experimentally by comparing stimulated-echo decay curves of our samples measured with RF flip angles optimized to 90° with decay curves measured with RF flip angles set to about 64° (reducing the RF power by 3 dB). The two sets of decay curves were found to coincide within experimental accuracy when a constant scaling factor was applied. These observations were corroborated by numerical simulations of the time evolution of the magnetization of a system of up to 10^6 spins. In these simulations the Bloch equations were solved in the presence of both longitudinal and transverse relaxation, pulsed RF fields, as well as diffusion in a uniform magnetic field gradient.

Before detailed measurements on a sample were started, both the primary and stimulated echoes was measured for a set of echo times below 10 ms. The RF power was adjusted such that the observed echo-time dependence of M_{st}/M_{pr} extrapolated to 1 for echo times going to zero. This adjustment was performed for each value of τ. Although this procedure is not required for the analysis of the echo decay, it has the advantage that no scaling factors have to be applied afterwards. An experimental advantage of using M_{st}/M_{pr} instead of M_{st} alone is that variations in the sensitivity of the receiver chain during these very time-consuming measurements are automatically compensated.

3. Experimental setup and materials

A home-built nuclear magnetic resonance apparatus was used. The operating frequency was 30.9 MHz ($B_0 = 0.7$ T). A constant magnetic field gradient was generated with a set of Anderson coils. The maximum gradient strength used in the experiments was 425 mT/m. A detailed description of the apparatus is given elsewhere [19].

The ratio of the amplitudes of the stimulated echo and the primary echo was measured as a function of the echo time, by changing the time interval between the second and third RF pulse (cf. Fig. 2) from 1 ms to 3 s. The complete set of data was obtained by varying the interpulse time τ and the applied external gradient G. The time τ was varied between 70 and 1000 μs, and the magnitude of G between 47 and 425 mT/m. The width of the RF pulses was 12 μs.

NMR diffusivity measurements were performed on porous samples of glass filter (Duran, borosilicate glass), fired-clay brick, and sintered crushed glass. The porosity of fired-clay brick is 23%. The pore sizes have been measured previously [20] and are in the range of 1–10 μm. The porosity of sintered crushed glass is 53% and the pore size measured by mercury intrusion amounts to 14 ± 3 μm. Glass filter is made from borosilicate glass. According to the supplier the pore sizes are in the range 10–16 μm. The measured porosity is 33%. Glass filter is used as a standard, magnetically 'clean,' material with pore sizes comparable to that of fired-clay brick and sintered crushed glass.

The samples have a cylindrical shape with a diameter of 2 cm and a length of 5 cm in the case of fired-clay brick and sintered crushed glass. The length of the glass filter sample was 6 mm. The samples were vacuum saturated with deionized water.

4. Results

4.1. Glass filter

As already mentioned above, this material contains a negligible amount of magnetic impurities. In Fig. 3A the measured ratio between the amplitudes of the stimulated echo and the primary echo is plotted semi-logarithmically against the spin-echo time t for various interpulse times τ at a constant gradient strength G. In Fig. 3B this ratio is plotted for various gradient strengths G at a constant τ. In all cases a mono-exponential decay is observed. The dashed lines represent fits of such decays to the experimental data. For all sets of data, the intercept of these fits with the vertical axis is given by $M/M_0 = 1$ within experimental inaccuracy, from which it can be concluded (Eq. (3)) that internal gradients are negligible. This suggests that the diamagnetic susceptibility of the solid pore matrix of this material is almost equal to that of water, which is present in the pore space. Within experimental accuracy, this is corroborated by the results of magnetization measurements presented in Table 2.

In order to determine the diffusivity we have plotted the slope $R = [1/T_1 + (\gamma G)^2 D\tau^2]$ of the fitted exponential decay as a function of $(\gamma G)^2\tau^2$ (see Fig. 6). Within experimental inaccuracy, a linear relation is found,

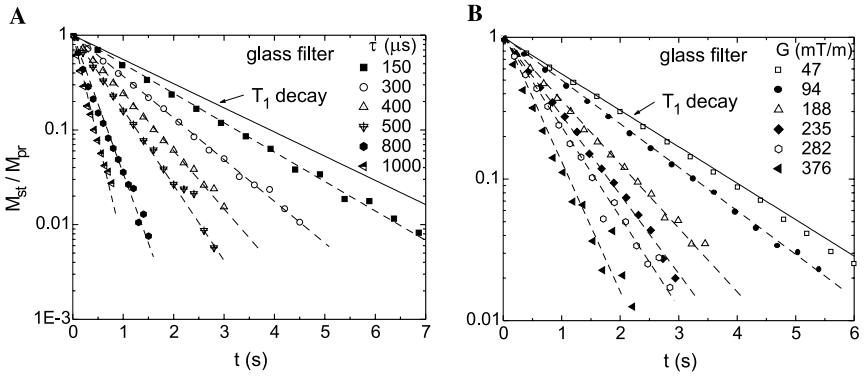

Fig. 3. Ratio between the stimulated echo and primary echo in a glass filter sample plotted against the spin-echo time. (A) τ is varied between 150 and 1000 μs at $G = 225$ mT/m, (B) G is varied between 47 and 376 mT/m at $\tau = 360$ μs. The solid line reflects the decay due to longitudinal relaxation only. Dashed lines are fits of a mono-exponential decay to the data.

indicating a constant diffusivity. This suggests that the water molecules are probing the complete pore space in the range of echo times t from 0.1 to about 5 s. The longitudinal relaxation time T_1 was measured independently by a saturation recovery sequence. The corresponding decay is reflected by the solid line in Fig. 3. The value of T_1 determined this way is in perfect agreement with the value determined from the intercept of R with the vertical axis in Fig. 6. The T_1 values and the diffusivity are given in Table 1.

Table 1
Comparison of the stimulated echo (SE) results with the values of T_1 obtained by the saturation recovery method (SR) and the electrolytically (EL) determined tortuosity α

	Glass filter	Sintered crushed glass	Fired-clay brick
T_1(s) (SE)	1.50 ± 0.02	0.36 ± 0.02	1.04 ± 0.02
T_1(s) (SR)	1.49 ± 0.01	0.37 ± 0.01	1.10 ± 0.02
D (10^{-9}m^2/s)	1.20 ± 0.05	1.55 ± 0.05	0.41 ± 0.02
α (SE)	1.8 ± 0.1	1.5 ± 0.1	5.6 ± 0.5
α (EL)	—	1.4 ± 0.1	5.9 ± 0.2

The thickness of the glass filter sample was insufficient to perform electrochemical tortuosity measurements.

4.2. Fired-clay brick and sintered crushed glass

Both fired-clay brick and sintered crushed glass contain a rather large amount of magnetic impurities [9,10]. In Figs. 4 and 5 the measured ratio between the amplitudes of the stimulated echo and the primary echo is plotted semi-logarithmically against the spin-echo time t for various τ (A) and gradient strengths G (B). Inspection of these figures shows that for both materials the decay is not mono-exponential. Only in the long time limit the magnetization decay can be described by a single exponent. Also for these materials, the value of T_1 has been determined independently by saturation recovery sequences.

There are two possible mechanisms which may explain the initial decay: diffusion in the internal gradients and diffusion in the external gradients. As the initial decay appears to be insensitive to the magnitude of the applied field gradient, at least in the range of G used in

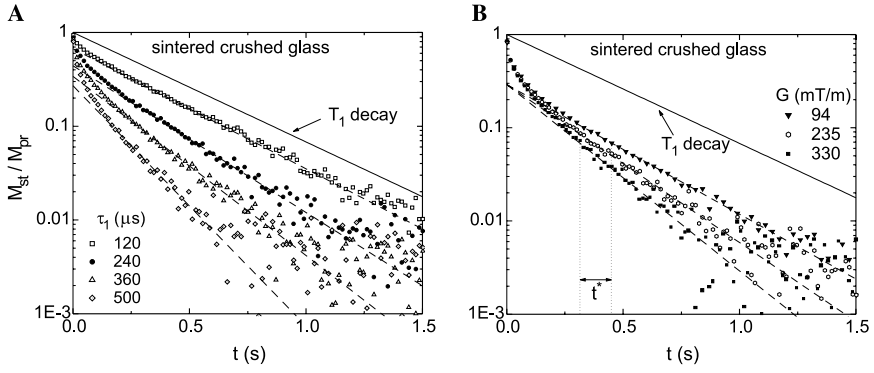

Fig. 4. Ratio between the stimulated echo and primary echo in sintered crushed glass plotted against the spin-echo time. (A) τ is varied at $G = 330$ mT/m. For clarity only the data for $t < 1.5$ s are plotted. (B) G is varied at $\tau = 410$ μs. The solid line reflects the decay due to longitudinal relaxation only. Dashed lines are fits of a mono-exponential decay to the data for $t > t^*$. The vertical dotted lines reflect the range of t^* for these experiments (see text).

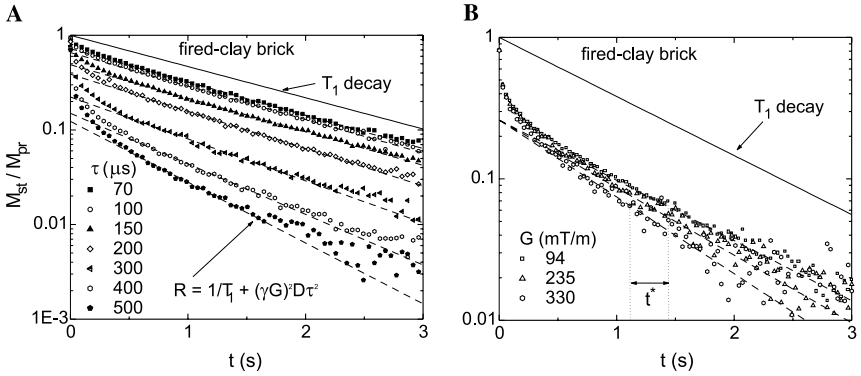

Fig. 5. Ratio between the stimulated echo and primary echo in fired-clay brick plotted against the spin-echo time. (A) τ is varied at $G = 188\,\text{mT/m}$. (B) G is varied at $\tau = 410\,\mu\text{s}$. See the caption of Fig. 4 for further explanation.

our experiments (see Figs. 4A and 5A), this decay is mainly caused by diffusion in the internal gradient fields, i.e., the water molecules feel a fluctuating magnetic field (Fig. 1). At longer time scales the external gradient strength has a significant effect on the signal decay, as can be seen from Figs. 4B and 5B. In order to improve the signal to noise ratio, a large number of signal averages was used (up to 300 in the case of fired-clay brick and 100 in the case of sintered crushed glass). It is obvious, however, that the noise cannot be neglected and has to be taken into account when fitting theoretical model predictions to the data. The magnitude of the noise was measured in a separate experiment and incorporated as a constant term in the fitting procedure.

By fitting the linear part of the decay curves with straight lines we observed that in the case of varying G (constant τ) the intersection $f(\tau) = -\gamma^2\tau^2\langle(\bar{B}_\tau)^2\rangle$ of these lines with the vertical axis is constant within experimental inaccuracy (Figs. 4B and 5B), whereas it changes significantly with varying τ (Figs. 4A and 5A). This agrees with the behavior predicted by our model (Eq. (3)).

The time at which the effects resulting from diffusion in external gradients become significant, t^*, is given by Eq. (4). It can be estimated from plots of $M_{\text{st}}/M_{\text{pr}}$ versus t from the time at which $R \times t^* = f(\tau)$. The range of t^* obtained this way is denoted by the dotted vertical lines in Figs. 4B and 5B. The diffusion coefficient can only be measured if the signal is still above the noise level for $t > t^*$. As already mentioned above, we had to use many signal averages to meet this condition.

In Fig. 6 the slope $R = [1/T_1 + (\gamma G)^2 D\tau^2]$ obtained from fits of straight lines to the data for $t > t^*$ is plotted against $(\gamma G)^2\tau^2$. Within experimental inaccuracy, a linear relation is found for both sintered crushed glass and fired-clay brick, indicating that the diffusivity does not depend on the observation time and the internal fields experienced by the spins have become uncorrelated. The fitted values of R for variations of both G and τ are located on a single line. The diffusivities and longitudinal relaxation times T_1 for both materials are given in Table 1. This table reveals that the values of T_1 obtained from Fig. 6 agree nicely with the values obtained from saturation recovery experiments.

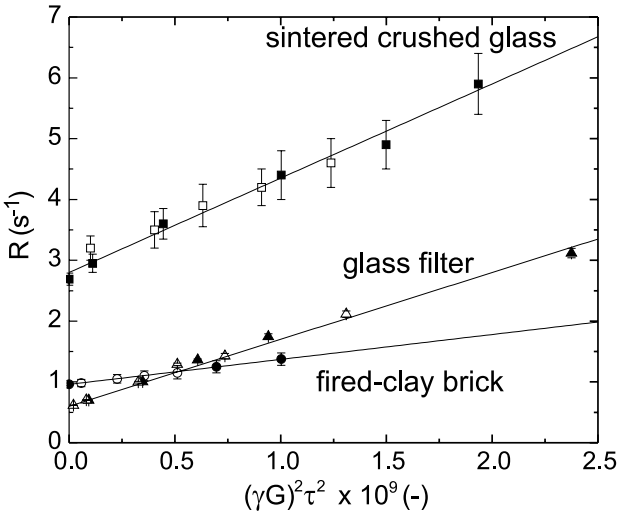

Fig. 6. Determination of the diffusivity and T_1 for the different materials. The values of R determined from the fits presented in Figs. 3–5 are plotted against $(\gamma G)^2\tau^2$. The data obtained at different values of G and at different values of τ are represented by open and solid symbols, respectively.

The tortuosity of the pore space is estimated from the long time behavior of the diffusivity (Eq. (1)). We measured the self-diffusion coefficient D_0 of bulk water by stimulated echo experiments. At 25 °C the measured value of D_0 is $(2.34 \pm 0.02) \times 10^{-9}\,\text{m}^2/\text{s}$, which is in good agreement with the literature value $(2.30 \times 10^{-9}\,\text{m}^2/\text{s})$ [21]. Tortuosities for the three samples are given in the Table 1.

As mentioned above, in the limit $\tau \to 0$ the term $\langle(\bar{B}_\tau)^2\rangle$ is equal to the squared standard deviation σ_B^2 of the internal field fluctuations. To estimate the magnitude of these fluctuations, we have plotted the intercept $f(\tau)$ of the lines fitted to the data for $t > t^*$ in Figs. 4A and

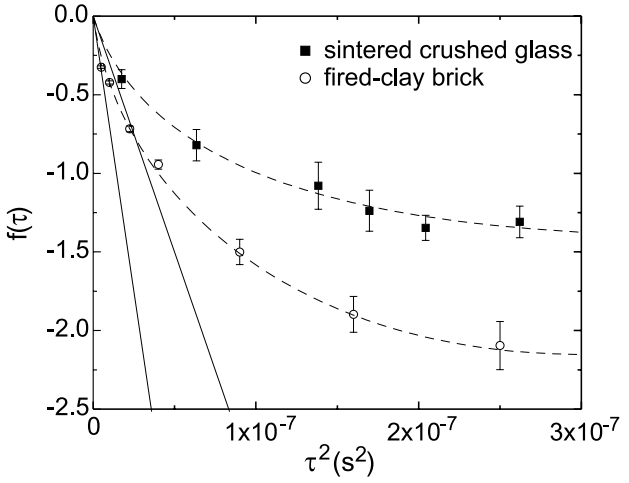

Fig. 7. Intercepts $f(\tau)$ of the fits presented in Figs. 4B and 5B plotted against τ^2. Dashed curves represent fits of a smooth function through the experimental values of $f(\tau)$. Solid lines reflect the estimated initial slope $-\gamma^2\langle(\bar{B}_\tau)^2\rangle$.

Table 2
Standard deviation of the internal field fluctuations σ_B determined by NMR, together with the amplitudes of internal magnetic fields ΔB_{int} obtained from bulk magnetization measurements

	Glass filter	Sintered crushed glass	Fired-clay brick
σ_B (μT)	0	25 ± 5	35 ± 5
ΔB_{int} (μT)	1 ± 1	25 ± 3	59 ± 6

All values of ΔB_{int} are the difference of the values obtained from the magnetization measurements on a completely dry sample and the value corresponding to a water–air interface at 0.8 T.

5A against τ^2. The results for both sintered crushed glass and fired-clay brick are presented in Fig. 7. One should note that, in principle, the location of the intercepts $f(\tau)$ may be affected by the procedure described in Section 2 to relate M_{st}/M_{pr} to $M(t)/M_0$. However, the possible error rapidly decreases for smaller values of τ, since in the limit $\tau \to 0$ no dephasing occurs. For this reason, a point $f(0) = 1$ has been added to the experimental data. The initial slope $-\gamma^2\sigma_B^2$ has been estimated from smooth curves through the data. The standard deviations σ_B obtained from this procedure are presented in Table 2.

5. Discussion and conclusions

We have demonstrated that in porous materials with a large amount of magnetic impurities the diffusivity of the pore fluid at long observation times (the tortuosity limit) can be measured from stimulated-echo experiments in static external gradient fields. The measured signal decay is interpreted in terms of a model (Eq. (3)) that describes the decay at times $t \gg t_B$, where the internal magnetic field fluctuations experienced by the diffusing spins at the start and the end of the observation time are uncorrelated.

The method presented in this paper may be useful for diffusivity measurements in many classes of materials in which internal magnetic fields interfere with the applied gradients (i.e., susceptibility induced fields in natural stones, inorganic, and biologic materials). In contrast to electrochemical measurements, the present method is also applicable to investigations of transport processes in unsaturated media, during drying, absorption, or crystallization.

One should note that the method can only be used in situations where the internal field fluctuations have become uncorrelated before the signal has dropped below the noise level, for instance, due to fast longitudinal relaxation. Attempts to determine the diffusivity of ^{23}Na ions in a fired-clay brick sample saturated with a NaCl solution did not succeed, because $T_1 \simeq 60$ ms for ^{23}Na in a bulk solution [22] and decreases even more in a porous material.

The standard deviation σ_B of the internal field fluctuations determined from the first term of Eq. (3) in the limit $\tau \to 0$ (Fig. 7) for sintered crushed glass and fired-clay brick is of the same order of magnitude as the amplitude of the internal field fluctuations (ΔB_{int}) determined from bulk magnetization measurements (Table 2). One should note that these magnetization data, which were obtained using a SQUID magnetometer, were analyzed assuming that the magnetic impurities are distributed homogeneously within the material. In that case the internal field fluctuations can be related directly to the maximum variation of the demagnetizing field at the pore to liquid interfaces [10]. Both magnetization and EPMA measurements [9], however, indicate that, especially in fired-clay brick, a fraction of these impurities is present in the form of small clusters, which act as localized magnetic dipoles. The internal fields in the direct vicinity of these dipoles may be much larger than the field variations arising from homogeneously distributed impurities, and hence the value of ΔB_{int} presented in Table 2 should be considered as a lower limit. Because of the presence of these clusters, the length scale of the internal field fluctuations ξ_B may also differ from the typical pore dimension d.

To investigate this point in more detail we focus on the behavior of the decay curves for $t < t^*$. We subtract the part of the decay that is dominated by the applied gradients (Eq. (3)) from the experimental data. As an example, the behavior of the remaining part $\lambda(t)$ for sintered crushed glass, $G = 188$ mT/m and $\tau = 400$ μs is plotted in Fig. 8. This figure shows that the part of the signal decay that can be attributed to the internal field fluctuations has vanished at $t \simeq 0.3$ s. This value would correspond to some characteristic time constant between 0.05 and 0.1 s.

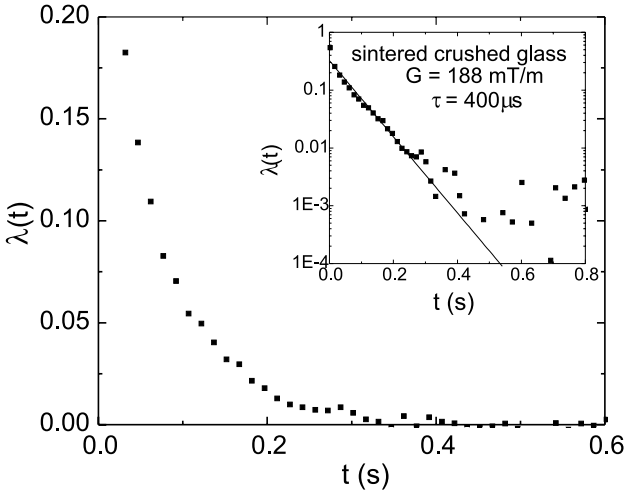

Fig. 8. Echo-time dependence of $\lambda(t)$, which represents the ratio between the stimulated echo and primary echo in sintered crushed glass minus the fitted long-time part of the signal decay. The inset shows a semi-logarithmic plot of $\lambda(t)$. The solid line in this inset reflects a fit of a mono-exponential decay to the data between 0.01 and 0.3 s.

To analyze the decay process more precisely, we plotted $\lambda(t)$ on a semi-logarithmic scale (inset of the figure). This plot suggests a mono-exponential decay, except for very short echo times. If we assume that, for constant G and τ, the decay M_{st}/M_{pr} can be factorized as $g(t)\exp(-t/T_1)$, the observed decay rate $1/T_d$ might be associated with a typical correlation time t_B according to

$$\frac{1}{T_d} = \frac{1}{t_B} + \frac{1}{T_1}. \tag{5}$$

This yields a correlation time $t_B = 80$ ms. This correlation time can be related to a typical length scale of the internal gradient fields using the expression $\xi_B = \sqrt{6Dt_B}$. The values of ξ_B for sintered crushed glass and fired-clay brick obtained this way are presented in Table 3.

For fired-clay brick, ξ_B seems to be significantly larger than the average pore size, which is in agreement with the presence a small amount of clusters of magnetic impurities. Because ξ_B is estimated assuming three-dimensional diffusion and the pore size r is obtained from a model-dependent interpretation of, e.g., mercury intrusion experiments, such a conclusion is not justified for sintered crushed glass.

Table 3
Typical time scales and correlation length scales ($\xi = \sqrt{6Dt}$) characterizing the three porous materials used in our experiments

	Glass filter	Sintered crushed glass	Fired-clay brick
t^* (s)	0	0.37 ± 0.07	1.3 ± 0.1
t_B (s)	0	0.08 ± 0.01	0.20 ± 0.02
ξ_B (μm)	0	27 ± 4	22 ± 3
d (μm)	10–16	14 ± 3	1–10

t^* is the time above which the effect of external gradients on the diffusion can be observed, t_B is the time related to the correlation length ξ_B of the internal field fluctuations, and d is the dominant pore size. In the glass filter sample no detectable internal field gradients are present (Section 4.1) and hence t^* and t_B have a value of zero.

It is obvious that our model does not give a complete description of the signal decay for $t < t^*$. One should note, however, that, except for t_B and ξ_B, all parameter values presented in this paper are obtained from the long time behavior of the signal decay, where details of the initial dephasing process of the spins are unimportant. The constant field gradient stimulated-echo NMR method, in conjunction with the model presented in this paper, provides a reliable method for the quantitative characterization of water transport in magnetically 'dirty' porous media (diffusivity), including the pore geometry of the media (tortuosity). We therefore intend to apply this method to investigations of macroscopic transport properties in building materials at different degrees of water saturation.

Acknowledgments

The authors thank R.M.E. Valckenborg for various stimulating discussions on the effect of large internal field gradients, J. Noijen for technical assistance with the NMR equipment, and J. Dalderop for the help in the preparation of the samples. We also acknowledge L. Janssen, M. Blijlevens, and L. Coene for the help with electrochemical impedance spectroscopy measurements, M. Geboers for the mercury intrusion measurement and C. Smits for the magnetization measurements. This work is supported by the Dutch Technology Foundation (STW).

Appendix A. Magnetization decay

Our aim is to measure the macroscopic diffusion coefficient D in 'dirty' porous media with the help of a stimulated-echo experiment. The long-time behavior of the echo decay in such an experiment contains information about this coefficient. In this appendix, we derive an expression for the echo decay on time scales $t > t_B$, when the pore space that is probed by the spins can be considered as homogeneous. The magnetization decay in a stimulated-echo experiment occurs via three different mechanisms: longitudinal relaxation (T_1), transverse relaxation (T_2), and dephasing. CPMG measurements on a glass filter sample revealed a perfect mono-exponential decay described by $T_2 = 0.65 \pm 0.02$ s. In similar measurements on sintered crushed glass and fired-clay brick always significant diffusion effects were present, even at the smallest attainable spacing between adjacent 180° pulses (150 μs). Nevertheless, these measurements clearly indicate that the value of T_2 in the latter two

materials exceeds 10 ms. Because in our stimulated-echo experiments the echo decay is measured for fixed time intervals $\tau \leqslant 500\,\mu s$ between the first and second 90° pulse, the effect of T_2 can be neglected. The mechanisms underlying longitudinal relaxation and dephasing are independent, and hence the magnetization $M(t)$ yielding the stimulated echo can be described by the following equation:

$$M(t) = M_0 \left\langle \exp(i\phi) \exp\left(-\frac{\zeta}{T_{1,S}}\right) \exp\left(-\frac{t-\zeta}{T_{1,B}}\right) \right\rangle. \tag{A.1}$$

In this equation t, M_0, $T_{1,S}$, and $T_{1,B}$ are the echo time, the initial magnetization, the longitudinal relaxation time of the spins in a boundary layer close to the pore wall, and the longitudinal relaxation time of the spins in the 'bulk' pore fluid, respectively. The quantities ϕ and ζ are properties of a group of spins that follow exactly the same path in space and time; ϕ and ζ are their phase angle and their total residence time near pore walls, respectively. Eq. (A.1) represents an ensemble average over all spins.

At the time scale of interest ($t > t_B$) the pore space probed by spins can be considered as homogeneous and all spins have the same residence time near the pore wall, $\zeta = t\lambda S/V$, where λ, S, and V are the thickness of the boundary layer, the pore surface, and the pore volume in the system, respectively [23]. For these time scales Eq. (A.1) can be rewritten as

$$\begin{aligned} M &= M_0 \langle \exp(i\phi) \rangle \exp\left[-t\left(\frac{1-\lambda S/V}{T_{1,B}} + \frac{\lambda S/V}{T_{1,S}} \right) \right] \\ &\equiv \langle \exp(i\phi) \rangle \exp\left(-\frac{t}{T_1} \right). \end{aligned} \tag{A.2}$$

The phase angle of a spin k, ϕ_k, can be calculated from:

$$\phi_k = \gamma \left[\int_{t-\tau}^{t} B(\vec{r}_k)\,dt - \int_0^{\tau} B(\vec{r}_k)\,dt \right]. \tag{A.3}$$

In this equation γ, B, τ, and $\vec{r}_k$ are the gyromagnetic ratio, the magnitude of the magnetic field, the time between the first two 90° pulses, and the position of spin k, respectively. The magnetic field experienced by a spin k consists of various contributions:

$$B(\vec{r}_k) = B_0 + x_k G_x + \tilde{B}(\vec{r}_k), \tag{A.4}$$

where B_0, G_x, and $\tilde{B}$ are the main magnetic field, the applied gradient (along x), and a fluctuating field, $\langle \tilde{B} \rangle = 0$, respectively. We only consider the component of the fluctuating field along B_0, which is allowed as long as $\tilde{B} \ll B_0$. Apart from this, we assume that any background gradients caused by, e.g., inhomogeneities of the main magnetic field or macroscopic demagnetization effects due to the non-spherical geometry of the sample, are very small compared to G_x. By combining Eqs. (A.3) and (A.4) we arrive at

$$\begin{aligned} \phi_k = \gamma G_x \left[\int_{t-\tau}^{t} x_k\,dt - \int_0^{\tau} x_k\,dt \right] + \gamma \left[\int_{t-\tau}^{t} \tilde{B}(\vec{r}_k)\,dt \right. \\ \left. - \int_0^{\tau} \tilde{B}(\vec{r}_k)\,dt \right] \equiv \phi_{k,G} + \phi_{k,B}, \end{aligned} \tag{A.5}$$

In this equation $\phi_{k,G}$ and $\phi_{k,B}$ are, respectively, used for the contributions of the applied gradient and the fluctuating field to the dephasing.

As already mentioned in Section 2, at time scales $t > t_B$ the spins experience a purely random field $\tilde{B}(\vec{r}_k)$, for which $\langle \tilde{B}(\vec{r}_k) \rangle = 0$. Hence $\langle x_k \tilde{B}(\vec{r}_k) \rangle$ will also be zero, which implies that $\phi_{k,G}$ and $\phi_{k,B}$ will be uncorrelated at time scales $t > t_B$. If we use this fact and substitute Eq. (A.5) in Eq. (A.2), we obtain

$$M \propto \exp(-t/T_1) \langle \exp(i\phi_G) \rangle \langle \exp(i\phi_B) \rangle. \tag{A.6}$$

The second term at the right-hand side of this equation is well known

$$\langle \exp(i\phi_G) \rangle = \exp(-\gamma^2 G^2 \tau^2 D t). \tag{A.7}$$

The last term at the right-hand side of Eq. (A.6) can be written as

$$\langle \exp(i\phi_B) \rangle = 1 - \frac{1}{2!} \langle \phi_B^2 \rangle + \frac{1}{4!} \langle \phi_B^4 \rangle + O(6). \tag{A.8}$$

Here O(6) represents terms of sixth and higher order in ϕ_B. It is important to note that $\langle \exp(i\phi_B) \rangle$ does not vary with time and only depends on the interpulse time τ. By using Eq. (A.5) we can obtain expressions for the terms at the right-hand side of this equation. For example, $\langle \phi_B^2 \rangle$ is given by

$$\langle \phi_B^2 \rangle = 2\gamma^2 \tau^2 \left\langle (\bar{B}_\tau)^2 \right\rangle, \qquad \bar{B}_\tau \equiv \frac{1}{\tau} \int_u^{u+\tau} \tilde{B}\,dt, \tag{A.9}$$

where the quantity $\bar{B}_\tau$ is the value of $\tilde{B}$ averaged over a time interval τ. Note that the ensemble average of this quantity is a function of τ when a significant dephasing occurs during the interval τ. In the limit $\tau \to 0$ this equation reduces to

$$\langle \phi_B^2 \rangle = 2\gamma^2 \tau^2 \left\langle \tilde{B}^2 \right\rangle = 2\gamma^2 \tau^2 \sigma_B^2, \tag{A.10}$$

where $\langle \tilde{B}^2 \rangle$ can also be thought of as the spatial average of $\tilde{B}^2$ and $\sigma_B \equiv \langle \tilde{B}^2 \rangle^{1/2}$ is the standard deviation of the field $\tilde{B}$. By combining the Eqs. (A.6), (A.7), and (A.9) we arrive at the following expression for the magnetization:

$$\begin{aligned} M = M_0 \left(1 - \gamma^2 \tau^2 \left\langle (\bar{B}_\tau)^2 \right\rangle + O(4) \right) \exp\left[-\left(T_1^{-1} \right. \right. \\ \left. \left. + \gamma^2 G^2 \tau^2 D \right) t \right]. \end{aligned} \tag{A.11}$$

For small values of τ this expression can be written as

$$M = M_0 \exp\left[-\gamma^2 \tau^2 \left\langle (\bar{B}_\tau)^2 \right\rangle - \left(T_1^{-1} + \gamma^2 G^2 \tau^2 D \right) t \right]. \tag{A.12}$$

This equation shows that by varying t, τ, and G systematically we are able to obtain the diffusion coefficient D and the magnitude of the internal fields σ_B. We wish

to note again that Eq. (A.11) is valid as long as $t > t_B$ and $\tau \ll T_2$, whereas Eq. (A.12) additionally assumes that τ is so small that no significant dephasing due to diffusion occurs during this time interval.

References

[1] J. Bear, Y. Bachmat, Introduction to Modeling to Transport Phenomena in Porous Media, Kluwer Academic, Dordrecht, 1990.

[2] R. Kimmich, NMR Tomography, Diffusometry, Relaxometry, Springer-Verlag, Berlin, 1997.

[3] M. Holz, S.R. Heil, I.A. Schwab, Electrophoretic NMR studies of electrical transport in fluid-filled porous systems, Magn. Reson. Imaging 19 (2001) 457–463.

[4] C. Vogt, P. Galvosas, N. Klitzsch, F. Stallmach, Self-diffusion studies of pore fluids in unconsolidated sediments by PFG NMR, J. Appl. Geophys. 50 (2002) 455–467.

[5] L.L. Latour, P.P. Mitra, R.L. Kleinberg, C.H. Sotak, Time-dependent diffusion coefficient of fluids in porous media as a probe of surface-to-volume ratio, J. Magn. Reson. Ser. A 101 (1993) 342–346.

[6] L.L. Latour, R.L. Kleinberg, P.P. Mitra, C.H. Sotak, Pore-size distributions and tortuosity in heterogeneous porous media, J. Magn. Reson. 112 (1995) 83–91.

[7] P. Wong, Experimental Methods in the Physical Sciences, Vol. 35: Methods in the Physics of Porous Media, Academic press, London, 1999.

[8] K.A. Snyder, X. Feng, B.D. Keen, T.O. Mason, Estimating the electrical conductivity of cement paste pore solutions from OH^-, K^+ and Na^+ concentrations, Cem. Concr. Res. 2260 (2002) 1–6.

[9] R.M.E. Valckenborg, NMR on technological porous materials, PhD thesis, Eindhoven University of Technology, 2000.

[10] R.M.E. Valckenborg, L. Pel, K. Kopinga, NMR relaxation and diffusion measurements on Iron(III)-doped kaolin clay, J. Magn. Reson. 151 (2001) 291–297.

[11] J.E. Tanner, Use of the stimulated echo in NMR diffusion studies, J. Chem. Phys. 52 (1970) 2523–2526.

[12] R.M. Cotts, M.R.J. Hoch, T. Sun, J.T. Markert, Pulsed field gradient stimulated echo methods for improved NMR diffusion measurement in heterogeneous systems, J. Magn. Reson. 83 (1989) 252–266.

[13] E.J. Fordham, S.J. Gibbs, L.D. Hall, Partially restricted diffusion in a permeable sandstone: observations by stimulated echo PFG NMR, Mag. Res. Imaging 12 (1994) 279–284.

[14] J.G. Seland, G.S. Sorland, K. Zick, B. Hafskjold, Diffusion measurements at long observation times in the presence of spatially variable internal magnetic field gradients, J. Magn. Reson. 146 (2000) 14–19.

[15] S. Vasenkov, P. Galvosas, O. Geier, N. Nestle, F. Stallmach, J. Karger, Determination of genuine diffusivities in heterogeneous media using stimulated echo pulsed gradient NMR, J. Magn. Reson. 149 (2001) 228–233.

[16] See, for instance D. Canet, Radiofrequency field gradient experiments, Progr. NMR Spectrosc. 30 (1997) 101–135, and references therein.

[17] Y.Q. Song, S. Ryu, P.N. Sen, Determining multiple length scales in rocks, Nature 406 (2000) 178–181.

[18] N. Nestle, A. Qadan, P. Galvosas, W. Süss, J. Kärger, PFG NMR and internal magnetic field gradients in plant-based materials, Magn. Reson. Imaging 20 (2002) 567–573.

[19] K. Kopinga, L. Pel, One-dimensional scanning of moisture in porous materials with NMR, Rev. Sci. Instrum. 65 (1994) 3673–3681.

[20] L. Pel, Moisture transport in porous building materials, PhD thesis, Eindhoven University of Technology, 1995.

[21] R. Mills, V.M.M. Lobo, Self diffusion in electrolyte solutions, in: Physical Sciences Data, 36, Elsevier, 1989.

[22] M. Eisenstadt, H.L. Friedman, Nuclear magnetic resonance in ionic solution. I. Relaxation of ^{23}Na in aqueous solutions of NaCl and $NaClO_4$, J. Chem. Phys. 44 (1966) 1407–1415.

[23] K.R. Brownstein, C.E. Tarr, Importance of classical diffusion in NMR studies of water in biological cells, Phys. Rev. A 19 (1979) 2446–2453.